Chapter 9
Uncertainty Quantification in Hydrodynamic Modeling Using the Example of a 2D Large-Scale Model of the River Elbe

Rebekka Kopmann, Sebastian Hudjetz, and Andreas Schmidt

Abstract Using a two-dimensional depth-averaged model of a 65 km long stretch of the River Elbe in Germany from Torgau to Wittenberg, methods for quantifying uncertainties are demonstrated and their benefit versus the required computational and analytical effort is discussed. In a first step, several input parameters like the friction parameters and the inflow discharges were assumed to be uncertain. The First Order Second Moment method was used to determine the most influential uncertain parameters. The influence of the most sensitive parameters on the model results was investigated in detail using Monte Carlo Simulations. The spatial distributions of the prediction interval and the failure probability visualize areas with uncertain or more reliable model results. Scatterplots and probability distributions at significant nodes illustrate the dependence of the results on uncertain parameters in more detail. Furthermore, the development of the uncertainties over time with regard to the hydrograph were analyzed and discussed.

Keywords Telemac-2D · Reliability analysis · FOSM · Monte-Carlo · Metamodeling · Scatter plots

9.1 Introduction

Multidimensional hydrodynamic modeling is a state-of-the-art tool in river engineering and is widely used at the German Federal Waterways Engineering and Research Institute (BAW). Within the last decades two-dimensional (2D) depth

R. Kopmann (✉) · S. Hudjetz · A. Schmidt
Federal Waterways Engineering and Research Institute, Kußmaulstraße 17, 76187 Karlsruhe, Germany
e-mail: Rebekka.kopmann@baw.de

S. Hudjetz
e-mail: sebastian.hudjetz@baw.de

A. Schmidt
e-mail: andreas.schmidt@baw.de

averaged modeling developed due to increasingly fast computations from small-scale models towards large model areas with fine grid resolution and long simulation periods. The simulation of a current river state and the prediction of the effects of river engineering measures are mostly possible with adequate reliability. However, a single simulation result does not consider the uncertainties due to natural variation or lack of knowledge in input parameters. In deterministic approaches input parameters must be fixed at a single value. Some parameters like roughness coefficients for floodplain vegetation cannot be described adequately with single values. The natural variation of that kind of input parameters pushes a deterministic approach to its limits. However, with increasing computational power, stochastic approaches are possible even for large scale 2D hydrodynamic models. With stochastic approaches it is possible to consider uncertainties of input parameters. Using these approaches the variations of these parameters can be described with statistic distributions instead of best fit values.

A central task of the BAW is the scientific investigation of river engineering measures on federal waterways on behalf of the Federal Waterways and Shipping Administration. The aim is to predict the effects of structural or operational measures on the waterways on hydraulic (discharge distribution, flow velocities, flow depths) and morphological and morphodynamic parameters (grain composition of the river bed, sediment transport). High demands are placed on the reliability of these predictions, as they represent essential elements in plan approval procedures.

In the context of morphological investigations, however, the results show considerable uncertainties, especially over long periods of prediction due to the inherently complex physical processes, the natural variation of the input and the system parameters and the inadequacies of the mathematical-numerical model. But it is not only in morphological investigations that uncertainty and reliability analyses can make a significant contribution to improving the evaluation of measures and their quality control. When missing measurements prevent proper calibration or the natural variability of a parameter is not considered by model functions, uncertainty quantification is also essential in hydrodynamic modeling.

In order to be able to evaluate the quality and significance of model simulation results, the following questions must be answered:

- Which uncertain parameters have the greatest impact on the simulated output parameters (e. g. water level, flow velocity)?
- How big is the influence on these output parameters?
- Which model areas are more (or less) uncertain?
- How does the uncertainty behave over time?

At BAW a tool was developed to integrate uncertainty quantification methods into project work [5]. In Chap. 2 of this paper the methods used in this tool are briefly described. The application of uncertainty quantification to a large Elbe model is presented in chapter 3. In chapter 4 results are presented and the benefits of uncertainty quantification in project work are discussed.

9.2 Uncertainty Quantification

With increasing computational power, the investigation of uncertainties for 2D hydrodynamic models became more and more popular (e.g. [9] or [1]). A good overview about uncertainty analysis in river modeling can be found in [11]. They state that in river modeling uncertainty analysis is an indispensable step and describe a methodology for it. According to [10], the potential deficit in the modeling process is defined as uncertainty if the reason is a lack of knowledge, or as error if it is not the lack of knowledge. With the uncertainty quantification the influence of the uncertainties to the model results is determined.

At BAW, a recently developed tool called UnAnToPy (**Un**certainty **An**alysis **To**ol in **Py**thon) supports users performing an uncertainty analysis of 2D river models. A procedure adapted to BAW requirements consisting of three steps was realized (see Fig. 9.1).

A detailed description of the method used in UnAnToPy can be found in [2]. In the following only a brief description of the procedure is given.

9.2.1 Initialization

First of all, the appropriate uncertain parameters must be selected depending on the model issues. Typically, input parameters that are not directly accessible to measurements and those that result from imprecise measurements are declared as uncertain. Additionally, parameters which have a natural variation can also assumed to be uncertain. The uncertain parameters should be statistically independent or the dependency between the parameters (joint probability distribution) must be known.

For each uncertain parameter a statistical description of its distribution is needed. In UnAnToPy six different distributions can be chosen each also as truncated distribution: uniform, normal, log-normal, exponential, gamma and beta. Dependent of
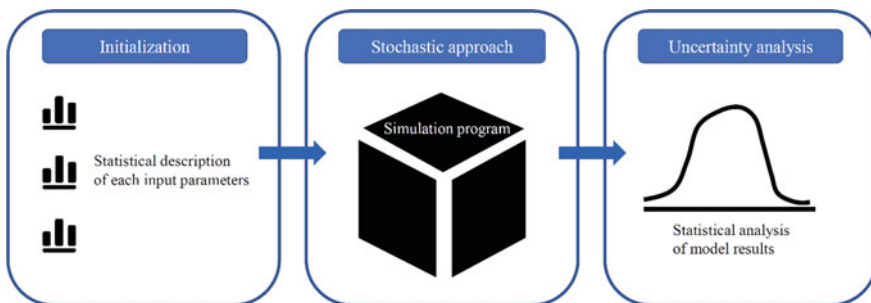

Fig. 9.1 Schematic diagram of the three steps of the uncertainty analysis tool UnAnToPy

the chosen distribution the statistical parameters mean value, standard deviation or truncation limits need to be given.

9.2.2 Probabilistic Approach

Three uncertainty quantification methods are implemented in UnAnToPy: First-Order Second-Moment (FOSM), Monte-Carlo Simulation (MC) and metamodeling (META).

The basis of the FOSM method is a Taylor series expansion which is truncated at the first order term. The variance of the output variable σ^2_{output} with respect to the standard deviation of the uncertain input parameters σ_{par_i} can be calculated (Eq. 9.1) on the assumption that the uncertain input parameters are statistically independent, the system behavior is linear and the input parameters are normally distributed.

$$\sigma^2_{output} = \sum_i \left[\frac{\partial output}{\partial par\_i} \sigma_{par\_i} \right]^2 \tag{9.1}$$

The sensitivity which is the gradient of the model output and the uncertain input parameters is computed by finite differences of two model runs. In case of centered gradients, the simulations with the mean value minus and plus the standard deviation of the uncertain parameters are used. The number of needed simulations results in twice the number of uncertain parameters. If the gradient is computed using forward or backward schemes, the number of needed simulation runs is reduced to the number of uncertain parameters plus one.

The probabilistic MC method is based on a large number of similar random experiments. Concerning the chosen distribution, the uncertain parameters are randomized and for each parameter set one simulation run is started. The standard deviation of the model results can be calculated with a statistical analysis of the model results. The number of experiments must be sufficiently large in order to ensure reliable results. UnAnToPy uses Latin Hypercube Sampling [3], which is a method to reduce the number of needed random experiments without compromising reliability. Comparing runs with different numbers of experiments serves to determine the appropriate number of experiments. For large scale models, this is often not a manageable procedure. Usually the number of experiments are chosen based on experiences with similar model settings. In addition, the results can be validated by comparing them with the results from metamodeling which achieves a better accuracy than MC using the same numbers of experiments.

Metamodeling is also based on a large number of similar random experiments like MC. Therefore, it is typically applied as an additional option to MC method. META is realized in UnAnToPy with the non-intrusive polynomial chaos (NIPC) method with the help of the OpenTURNS package of Python. The MC simulation runs were

Table 9.1 Comparison of uncertainty quantification methods in UnAnToPy

Uncertainty quantification methods	Advantages	Disadvantages	Typical applications
FOSM	• Small number of simulation runs	• Requirement of linear system behavior in the range of parameter deviation • Only Gaussian distribution for uncertain parameters • Requirement of statistical independency of parameters	• Determination of most sensitive parameters • Determination of qualitative behavior of the uncertainty influence in model outputs • Determination of reliable / non-reliable regions
MCS	• No requirements for the probability distributions of uncertain parameters • No assumption of system behavior is required	• Large number of simulation runs	• Determination of quantitative behavior of the uncertainty influence in model outputs • Determination of dependency between uncertain parameter and model result
META	• No requirements for the probability distributions of uncertain parameters • No assumption of system behavior is required • One order of magnitude less simulation runs than MC	• Large number of simulation runs • Additional approximation due to use of Polynomial Based on results from the FOSM method, Chaos functions	• Determination of quantitative behavior of the uncertainty influence in model outputs • Determination of dependency between uncertain parameter and model result

used to fit the polynomial chaos functions which replace the costly simulation runs. Additional runs with the META method increase the accuracy of the statistical results.

Further details of the methods can be found in [2]. Table 9.1 shows the advantages and disadvantages and typical applications of the uncertainty quantification methods of UnAnToPy.

9.2.3 Uncertainty Analysis

Based on results from the FOSM method, the sensitivity of each uncertain input parameter and the standard deviation of the output variables can be computed with

Eq. 9.1. Whereas both the MC and META methods offer more evaluation possibilities. The model results of all random experiments N can be statistically analyzed regarding e.g. mean values, standard deviations and other statistical values of the output variables.

In addition, data visualization as scatterplots offers the possibility to show the distribution of all random experiments at a (representative) node and to further examine the behavior of the model. A scatterplot visualizes the relative importance of the uncertain parameters with the standardized regression coefficient describing the correlation between two parameters. Furthermore, probability distributions of the output variables indicate the system behavior at selected nodes. This allows to verify the necessary assumptions for the FOSM method and is helpful for further understanding of the system.

9.3 Case Study Elbe

9.3.1 The Elbe Model

At the River Elbe the BAW operates a 65 km long 2D hydrodynamic model between Torgau and Wittenberg to investigate different river bed and floodplain measures (Fig. 9.2). After approx. 45 km the River Elster flows from the right into the River Elbe. Dikes define the lateral boundaries of the model area which comprises approx.
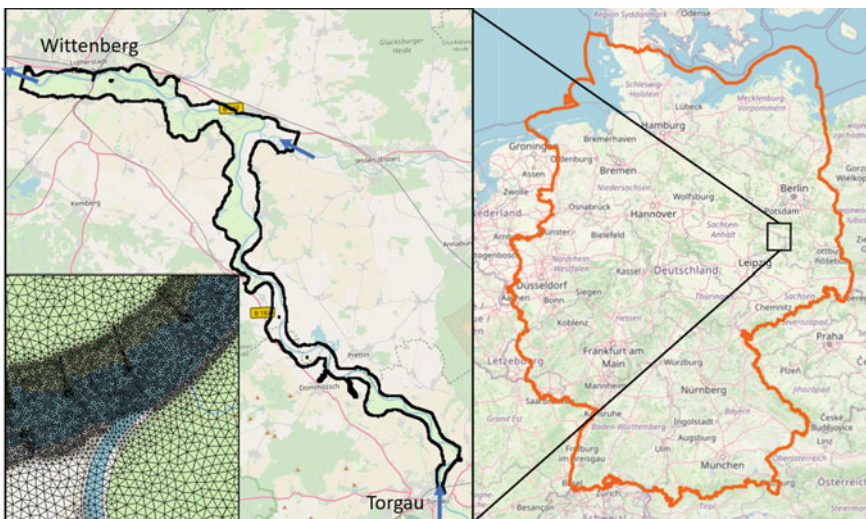

Fig. 9.2 Model area and details of discretization. Blue arrows depict flow direction. © Open-StreetMap contributors

91.5 km^2 and can be roughly divided into an upstream and a downstream region. The upstream region is characterized by small floodplains and several bottlenecks which lead to comparably high water depths during flood events. The downstream region, on the other hand, includes wide floodplains with numerous abandoned channels which distribute high water discharges over the whole river foreshore.

For the simulation the open source software Telemac-2D (opentelemac.org) was used. The model geometry was based on a digital terrain model and discretized with nearly 1.4 million triangles. The mean node distances varied from about 6 m in the main channel to up to about 20 m on the floodplains (Fig. 9.2). In order to precisely depict the groyne geometry a minimum node spacing of 1 m was sufficient. At the upstream boundary of the model area the Elbe discharge was used as boundary condition and the Elster discharge at the Elster inlet respectively, while the water level was used as boundary condition at the downstream boundary of the model area. The flow direction is from south to north.

The model was calibrated using 31 different roughness zones for discharges between low water discharge and high flood discharge [7]. Mainly Nikuradse friction law was applied except for forests and buildings for which the Lindner & Pasche approach [6] was used. Figure 9.3 shows the different roughness zones with the
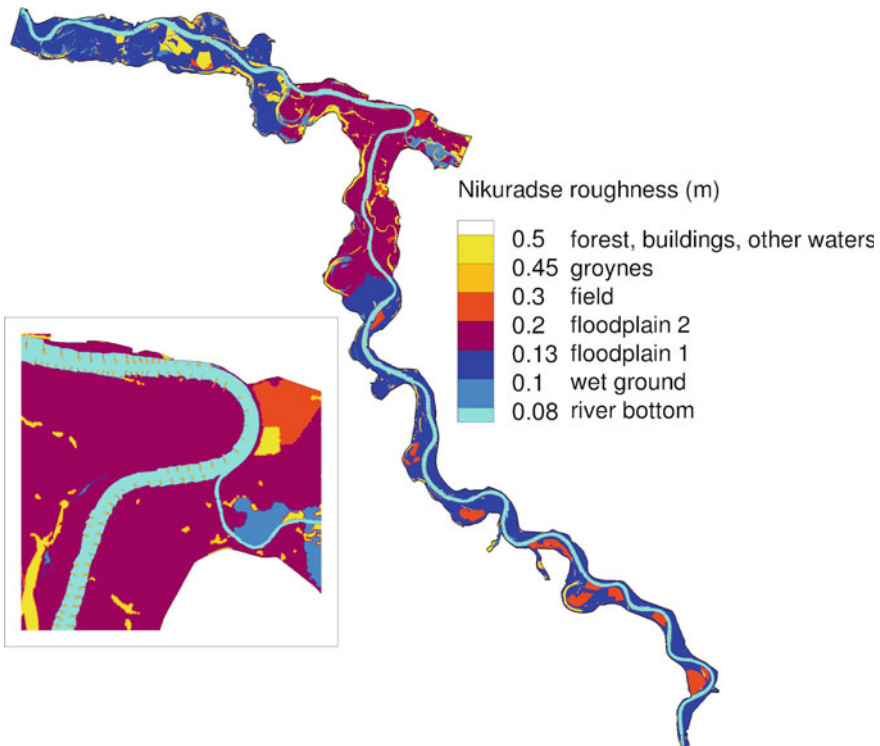

Nikuradse roughness (m)

0.5   forest, buildings, other waters
0.45   groynes
0.3   field
0.2   floodplain 2
0.13   floodplain 1
0.1   wet ground
0.08   river bottom

Fig. 9.3 Distribution of roughness zones

category «river bottom» combining all 22 zones of river bottom roughness with equivalent sand roughness coefficients between 4 – 8 cm. As turbulence model the horizontal mixing model was chosen.

9.3.2 Uncertain Parameters

In a first step all friction parameters and the inlet discharges for Elbe and Elster were considered uncertain which resulted in a total of 12 uncertain parameters. For each parameter a Gaussian distribution was assumed to describe the uncertainty. Table 9.2 shows the mean values from the calibration and the chosen standard deviations for each uncertain parameter. The standard deviation for the discharges were set 2% for discharges up to mean flood and 5% for discharges above. This is within the

Table 9.2 Uncertain parameters

Uncertain parameters	Mean value	Standard deviation
Inflow Elbe (m^3/s)	346 … 2875	2% up to mean flood discharge 5% > mean flood discharge
Inflow Elster (m^3/s)	20 … 60	4% up to mean flood discharge 10% > mean flood discharge
Nikuradse roughness floodplain 1 (m)	0.13	0.013
Nikuradse roughness floodplain 2 (m)	0.2	0.02
Lindner Pasche distance forest (m)	2.5	0.25
Lindner Pasche distance buildings (m)	3	0.3
Nikuradse roughness fields (m)	0.3	0.03
Nikuradse roughness wet ground (m)	0.1	0.01
Nikuradse roughness bridge piers (m)	0.02	0.002
Nikuradse roughness river bottom (m)	0.04 – 0.08	0.002 – 0.004
Nikuradse roughness other waters (m)	0.5	0.05
Nikuradse roughness groynes (m)	0.45	0.045

range given in literature (e.g. [8]). The chosen Elster discharge is not based on direct measurements, but derived from measurements taken at a distance. Thus, the standard deviation of the Elster inflow is doubled to 4 resp. 10%. In the calibration process, the river bottom roughness coefficients are usually the most sensible. Preserving the calibration could only be done assuming a moderate standard deviation for these values.

Therefore, a standard deviation of 5% was chosen while the standard deviation of all other roughness coefficients was set to 10%. This reflect the lack of calibration data for higher water levels, the high natural variation of vegetation and the fact that there are a lot of possible roughness coefficients combinations at the floodplains. But the 10% does not consider the full natural variability of floodplain vegetation which is not the aim of this uncertainty analysis.

9.3.3   Investigations

9.3.3.1   Steady State Investigations

The influence of the 12 uncertain parameters to the model results were firstly investigated at steady state conditions firstly. Three discharges were chosen from mean-flow conditions to flood conditions in order to cover the most important discharge range: Mean water discharge (MQ), mean flood discharge (MHQ) and 5–10-year flood discharge (HQ5). The sensitivity and the influence of each of the 12 uncertain parameters to the outputs were investigated with FOSM. From these results the most influential parameters were selected and used for further analysis.

For the mean flood discharge the methods MC and META were applied to verify qualitatively the FOSM results and to obtain more details about the system behavior and the influence of the uncertain parameters on it.

9.3.3.2   Artificial Flood Event

From the steady state investigations, the most influential uncertain parameters were selected: Elbe inflow, Nikuradse roughness for floodplain 1, floodplain 2, river bottom, other waters and groynes. An artificial flood event (Fig. 9.4) based on a natural flood event in 2006 was constructed. The hydrograph is characterized by 28.5 flood days followed by a steady state of 11.5 days. The development over time of the influence of the 6 uncertain parameters to the model results were investigated with the FOSM method.
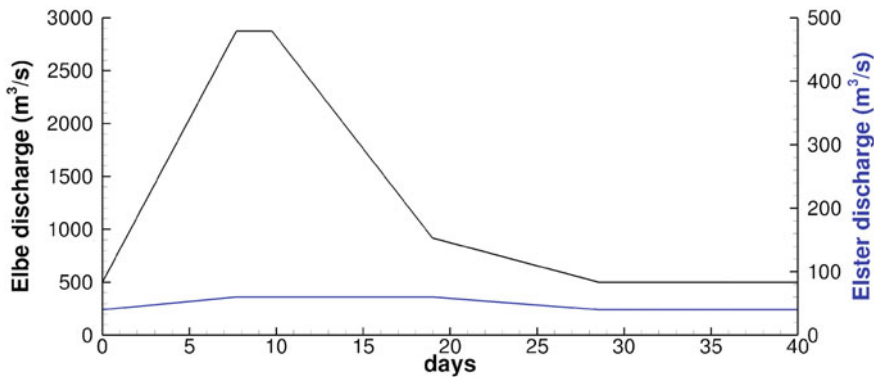
Fig. 9.4 Artificial flood event

9.4 Results and Discussions

9.4.1 Steady State Investigations Using FOSM Method

The influence of an uncertain parameter to the model results is not only determined by its sensitivity but also by its standard deviation. This influence is visualized in the following by the standard deviation of the output parameter. The water level is used as output parameter as it is an integral parameter with a smooth behavior in space and time. The standard deviation of the water level will be zero at the downstream model boundary due to the fixed water level as boundary condition. Thus, there is a general increasing trend of the standard deviation from the downstream to the upstream boundary.

Figure 9.5 shows the standard deviation of the water level along the river axis for the most influential uncertain parameters and three discharge scenarios (MQ, MHQ, HQ5). The parameters are called most influential if they induce more than 1 cm of standard deviation in one of the steady state situations. This is only the case for the Elbe discharge and the roughness coefficients for the river bottom and the floodplain 1 and 2. While the influence on the roughness coefficient for river bottom decreases with increasing discharge, the influence on the floodplain roughness coefficients increases with increasing discharges, since the decisive factor here is that more regions are covered with increasing runoff. Not surprisingly, the Elbe discharge causes the largest standard deviations of the water level for all three steady state situations. It is the only parameter which induces larger standard deviations than 5 cm.

Due to the chosen smaller standard deviation of the discharge for mean (MQ) and mean flood discharge (MHQ), the standard deviation of the water level is very moderate with a maximum of 7 / 10 cm at the inflow boundary and less than 1 cm
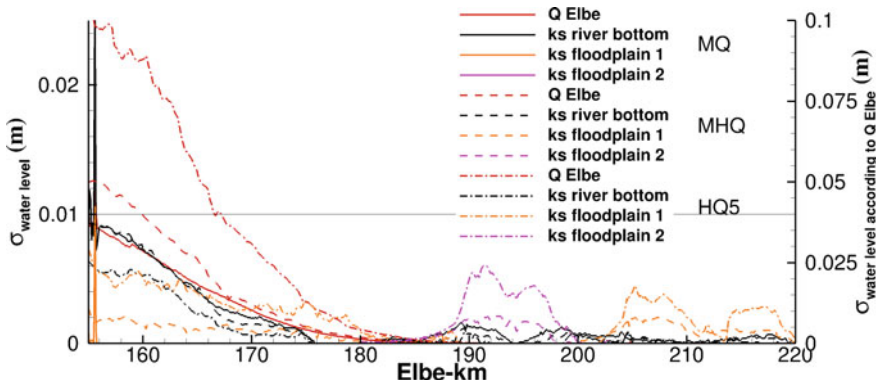
Fig. 9.5 Water level standard deviation along the river axis according to the most influential uncertain parameters for mean discharge (solid lines), mean flood discharge (dashed lines) and 5–10-year flood discharge (dashed dotted lines)

downstream from El-km 175. The expansion of the influence in river length is equivalent for mean and mean flood discharge but larger for the 5–10-year discharge due to the increased standard deviation from 2 to 5%.

Figure 9.6 shows the standard deviation of the water level according to the Elbe discharge for all investigated discharges as surface plots. The white areas indicate water depths less than 10 cm. It can be seen that most of the model region is overtopped for the 5–10-year flood. The differences across the flow direction are negligible for mean and mean flood discharges. Small deviations can be seen for the 5–10-year flood discharge (Fig. 9.6 bottom right).

Figure 9.7 shows the standard deviation of the water level according to all chosen uncertain parameters along the river axis for the mean discharge. In addition to the most influential parameters discussed before, the small influence due to the Elster discharge—up and downstream the Elster confluence at El-km 198 - can be seen. The effect of groyne roughness is also shown. The instabilities at El-km 155.6 which are visible in the standard deviation according to the Elbe discharge, the river bottom and groyne roughness, are caused by not optimal boundary conditions at mean discharge. In case of smaller water levels, the cross section at the inflow boundary is not fully compact. A second flow chain is formed on the right outer side of the cross section, which connects the main flow over an area with low water levels. The shallow part is responsible for the instabilities at El-km 155.6. This is a good example that uncertainty quantification is also able to highlight the numerically weak regions of a model.

Figure 9.8 shows the spatial distribution of the standard deviation of the water level according to the roughness coefficients for floodplain 1 and 2. Notable is that an increase of roughness induces increasing water levels at the same regions (El-km 155–183 and 205–220 for floodplain 1 and El-km 190–200 for floodplain 2) but decreasing water levels in the downstream regions (El-km 190–200 for floodplain 1 and El-km 205–200 for floodplain 2).
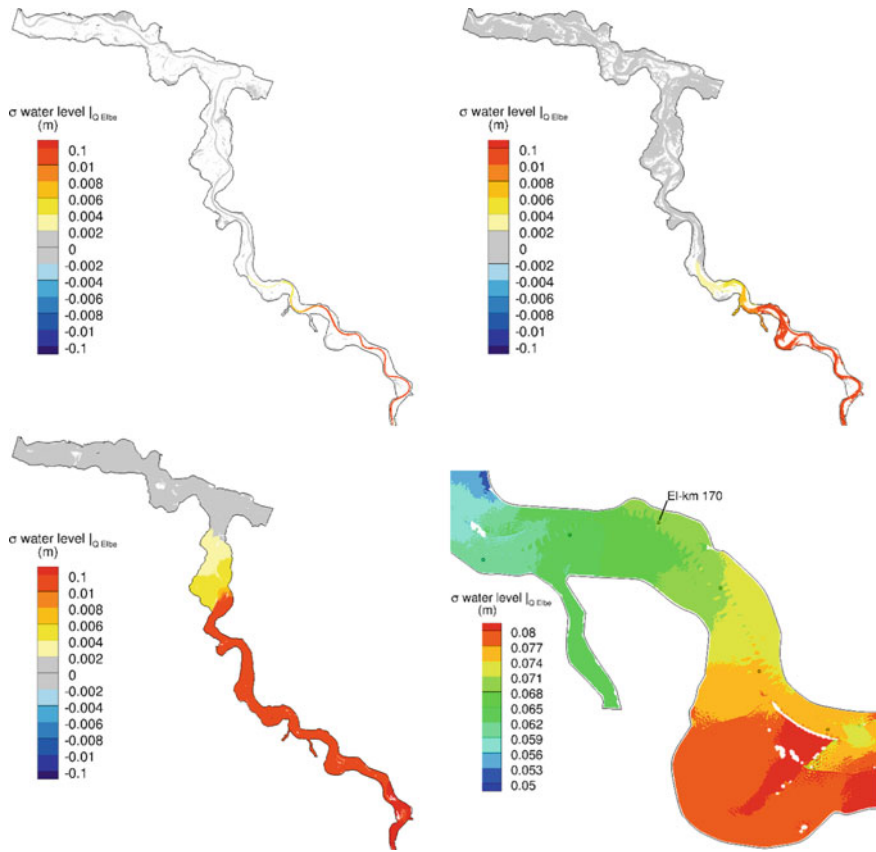
Fig. 9.6 Water level standard deviation according to Elbe discharge for mean discharge (top left), mean flood discharge (top right) and 5–10-year flood discharge (bottom left, detail: bottom right)

Generally, it can be stated that the chosen uncertainty does not affect the model results significantly except for the Elbe discharge in the case of a 5–10-year flood event. Thus, the model calibration can be considered very robust concerning the chosen (small) uncertainty in the input parameters and is therefore well suitable for forecasting. The geometry of the model inlet and thereby the upstream boundary condition should be modified to avoid instabilities at mean discharge. This will improve the local accuracy of the model.

For the steady state discharges, all simulations were started from a previous computation file including the steady state of the calibrated model. The adaptation according to the slight changes of the uncertain parameters did not need much simulation time. Investigations showed that a steady state was reached after 2 h resp. 4 h simulation time for the highest discharge. The computing time for one simulation run on a parallel cluster at BAW using 256 cores needed depending on the discharge approx. 2 / 2.5 / 5.5 min. The FOSM method with centered gradient calculations
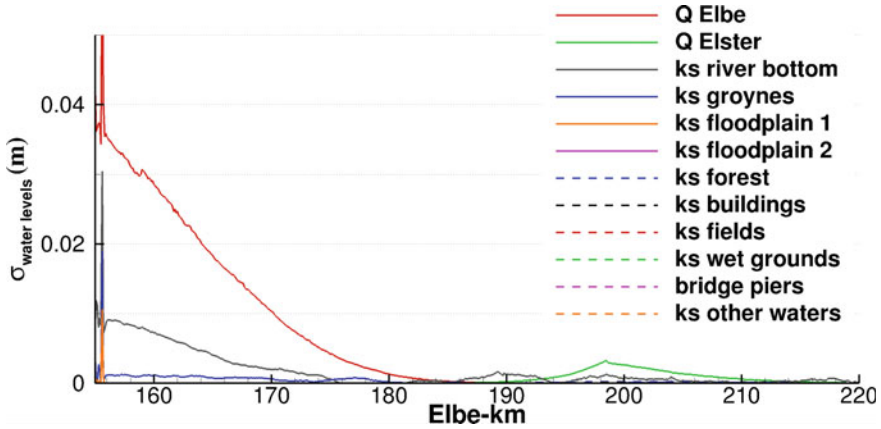
Fig. 9.7 Water level standard deviation along the river axis according to all uncertain parameters for mean discharge
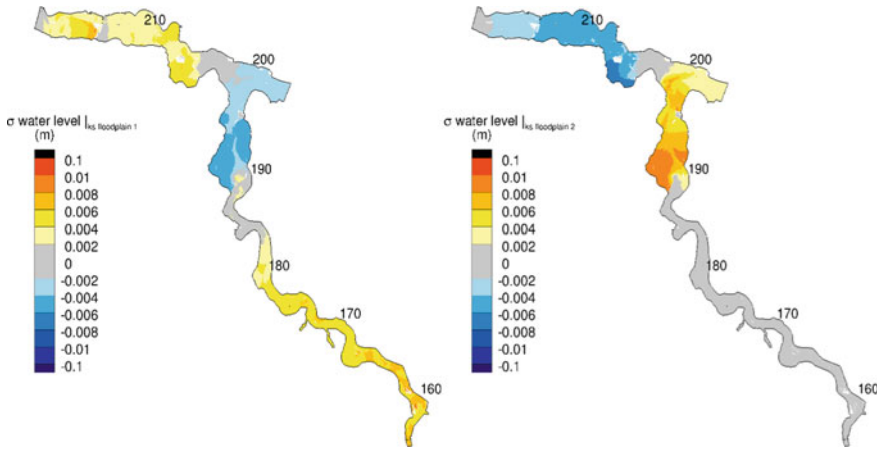

Fig. 9.8 Water level standard deviation according to roughness of floodplain 1 (left) and floodplain 2 (right) at 5–10-year flood discharge

required 33 simulation runs for each discharge scenario. The overall computing time for the steady state investigations using FOSM was 5.5 h.

9.4.2 Steady State Investigations Using the MC Method

With the MC method the combined uncertainty of all significant parameters was investigated for the mean flood discharge. For this analysis, 100 and 1000 samples
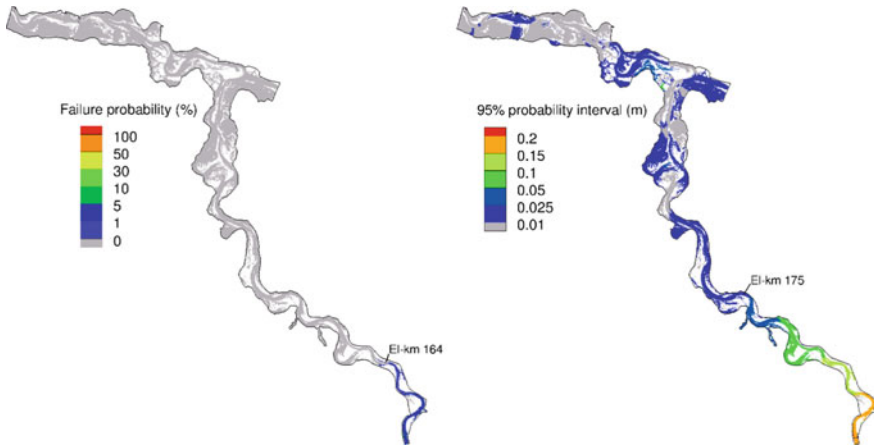
Fig. 9.9 Failure probability of the water level for the range $\pm$ 0.05 m of the calibrated value (left) and 95%-probability interval of the water level (right)

were used to verify if that the smaller number is sufficient. The deviations of the results between 100 and 1000 samples were less than 10%. Nevertheless, the results used in this paper are based on 1000 samples because of the higher accuracy, especially for the scatter plots. For further investigations with similar models 250 or 500 samples are recommended.

In addition to the most influential parameters found with the FOSM method (see Sect. 9.4.1: Elbe discharge, roughness coefficients of river bottom, floodplain 1, floodplain 2), the roughness coefficients for forest, groynes and other waters were investigated. Figure 9.9 on the left shows the failure probability that the water level is out of the range $\pm$ 5 cm of the calibrated value. According to the results of the FOSM method, even the combined uncertainty is negligible for most of the model region. Only at the inlet boundary a 5% probability was computed that the deviation according to the uncertain parameters is above $\pm$ 5 cm. This probability decreases to less than 1% at approx. El-km 164. This means that the influence of the chosen uncertainty to the input parameters can be neglected in the vicinity of the model inlet. The 95% probability interval is shown in Fig. 9.9 on the right. From El-km 175 downstream, the impact of the uncertain parameters is less than 2.5 cm with a probability of 95%. With this evaluation, the differences between the regions concerning the reliability of simulation runs can distinguished more clearly.

Furthermore, segments of 5 km length along the river axis were chosen to compute scatterplots and standardized regression coefficients (SRC). With the scatterplots and the calculation of the SRC, the relative importance and the existence of a linear relation between the uncertain parameters and the simulation results can be shown. SRC values above 0.5 imply a significant relative importance of the uncertain parameter. The scatterplots in Fig. 9.10 plot the simulated water level values for each sampled Elbe discharge at exemplarily chosen nodes along the river axis. The scatterplots until El-km 175 show a distinct correlation between Elbe discharge and water level with
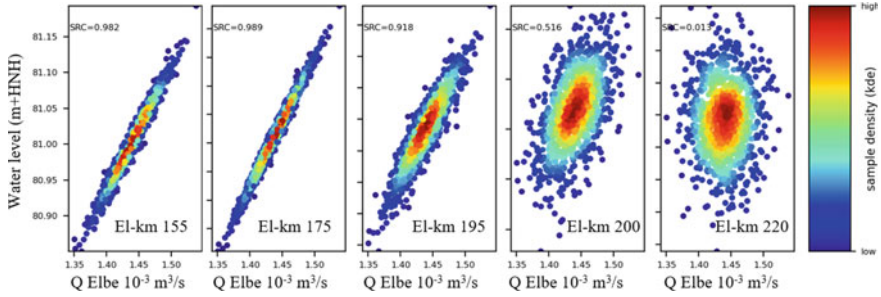
Fig. 9.10 Scatterplots water level according Elbe discharge for nodes at the river axis at El-km 155, 175, 195, 200 and 220

SRC values near 1. Further downstream the relative influence of the Elbe discharge decreases up to zero (SRC values near 0). For the first 20 km (El-km 155 - 175) the Elbe discharge dominates the results and consequentially the SRC values of the other parameters are very low.

From El-km 180 downstream, the roughness parameters of the river bottom and the floodplains are decisive. In Fig. 9.11 scatterplots with SRC values above 0.5 are plotted. During calibration, the river bottom was divided into 22 roughness zones using Nikuradse roughness from 4 to 8 cm. For the MC investigation, the zones
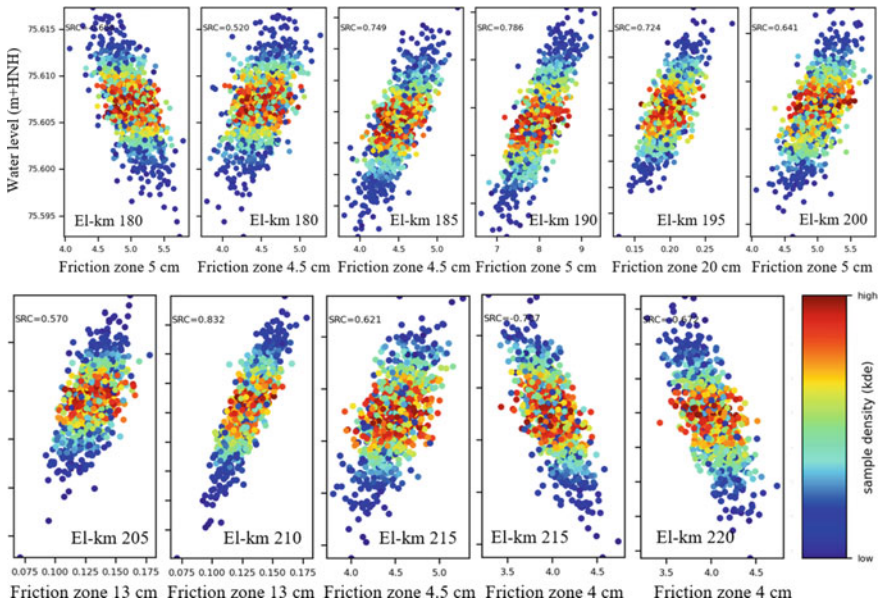

Fig. 9.11 Scatterplots of water levels according roughness coefficients (river bottom friction zones 4 cm – 5 cm, floodplain friction zones 13 and 20 cm) for nodes at the river axis from El-km 180 (top left) to 220 (bottom right)
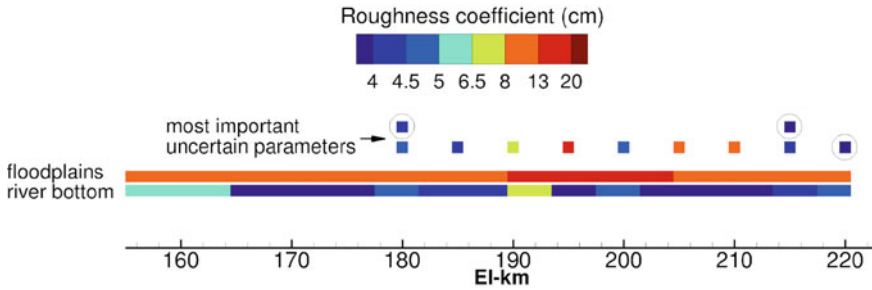
Fig. 9.12 Roughness coefficients of river bottom and floodplains along the river axis together with the position of the most important parameter given in the scatterplots in Fig. 9.11

with the same value were combined resulting in 5 river bottom zones with roughness coefficients of 4 (zone 13), 4.5 (zone 11), 5 (zone 10), 6.5 (zone 9) and 8 (zone 12) cm. Zone 9 has no significant impact as it is located near the inflow boundary where the Elbe discharge has the biggest impact.

Figure 9.12 shows the arrangement of the river bottom and floodplain roughness zones together with the position of the most influential roughness zones. For almost all sections, the uncertainty of the respective roughness zones has a direct effect on their position and with a typical proportional behavior. But at El-km 180, the uncertainty of the downstream roughness zone and at El-km 215 and 220 the uncertainty of the upstream roughness zone also affects the section. In these cases, the influence of the roughness coefficients is inversely proportional to the water level. A similar behavior was already detected in Sect. 9.4.1 Fig. 9.8.

The analysis with scatterplots provides detailed information about the impact of the investigated parameters on the simulation results. This knowledge can accelerate a calibration process or can help evaluate river engineering measures.

The probability distributions for the output results at specified nodes can be computed from the statistical analysis by the MC method. The analysis was done for nodes at the river axis each 5 km. Figure 9.13 shows the probability distribution
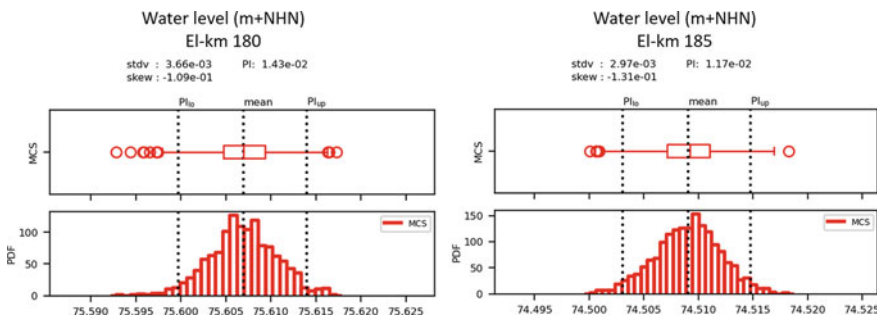

Fig. 9.13 Probability distribution function of the water level and the statistic values for two chosen nodes at the river axis

functions (PDF) and the statistic values for the water level at two chosen nodes at
the river axis. The nodes were selected because the mean value of the PDF fits best
(Fig. 9.13 left) or worst (Fig. 9.13 right) to the calibration result (black dotted line).
Even the worst node does not differ significantly from the calibrated value, which
indicates a linear system behavior. This is also confirmed by the computed PDFs
which could be roughly called Gaussian distributed. The requirement of a slightly
linear system behavior for the FOSM method can be proofed hereby.

9.4.3   Investigations of Artificial Flood Event

The investigations were done with the FOSM method as one simulation run needed
approx. 18 h. For all 6 uncertain parameters and centered gradient computation the
computing time was 234 h. Figure 9.14 shows the development over time of the
standard deviation of the water level according to all uncertain parameters every
5 km at the river axis from El-km 165 to 220. The influence of the Elbe discharge
is approx. 10 times larger than for the other uncertain parameters so that the second
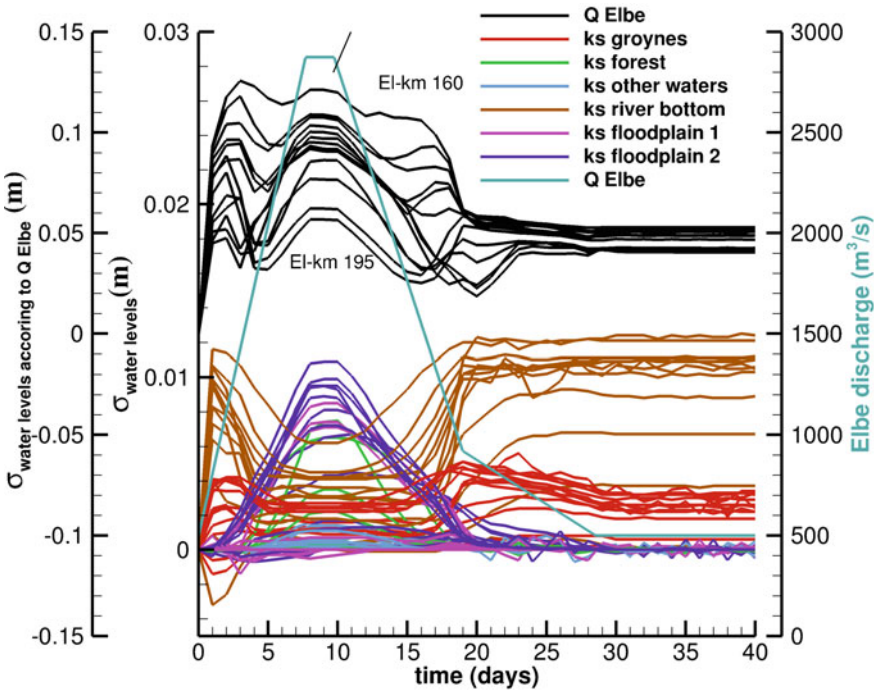y-axis was used.

Fig. 9.14 Time evolution of the standard deviation of the water level according to all uncertain
parameters every 5 km at the river axis (El-km 165 to 220)

A main difference to the steady-state simulations of Sect. 9.4.1 and 9.4.2 is that a stage discharge curve was imposed at the downstream boundary. Therefore, the influence of the uncertainties at the downstream boundary does not decrease to zero. The standard deviations of the water level show a strong correlation to the inlet discharge for all uncertain parameters. The influence of the uncertain parameters remains almost constant after 28.5 days according to the inlet discharge. Again, the most influential parameter is the Elbe discharge. All other parameters induce a standard deviation of the water level of less than 1.5 cm. Remarkably, the uncertainty of roughness of the river bottom and groynes leads to a decrease of the standard deviation of the water level during high floods. Maximum values are reached at the minimum discharge for the river bottom roughness and at approx. 1100 m^3/s for groynes. The reason is a reduced effectiveness of roughness because of high water levels. As groynes are generally higher than the river bottom, the maximum occurs at higher discharges. The simulation started from a steady state with a discharge of 500 m^3/s while the standard deviation started from zero. The strong increase and the first peak of the standard deviation after 1 day was related to this discrepancy.

The analysis of the artificial flood event confirms that uncertainties in hydrodynamic simulation are correlated with the flow dynamics. In contrast to morphodynamic simulations [4] no delay or aggregation of uncertainty can be observed. Therefore, the analysis of steady state situation seems to be sufficient as long as the objective of the study is not highly linked to flow development over time like e. g. investigations of retention effects.

9.5 Conclusions

The presented uncertainty analysis for a 65 km long 2D hydrodynamic model of the Elbe river shows the knowledge gain achieved with such a procedure for reasonable computing time. From a large number of uncertain parameters, the most influential ones were identified by the FOSM method. The results of this method are not necessarily quantitatively accurate but deliver a good and fast overview of the effects of each uncertain parameter on the model results. The most influential parameters were analyzed in more detail by the MC method. This method is much more expensive in terms of computing time, but offers more accurate and detailed results.

For the selected 12 uncertain parameters, comparatively small standard deviations between 2 and 10% of the calibrated values were assumed to cover the effect of other equally reasonable calibration configurations. Three steady state situations (mean discharge, mean flood discharge and 5–10-year flood discharge) were analyzed using the FOSM method. With the exception of the Elbe discharge, the impact of the uncertain parameters (roughness coefficients and the Elster discharge) was found to be negligible for all discharges. This result shows that the model is robust to small changes and can therefore be used for predictions.

In addition, instability at the model inlet was found for the mean flow discharge. This is a typical (side) effect of uncertainty quantification, which highlights the numerically weak regions of a model.

A more detailed analysis was carried out using the MC method for the mean flood discharge. This required 1000 simulation runs, which needed 30 times more computing time for one steady state situation than FOSM. The probability interval provided quantitative information about the reliability of the model results. According to the FOSM results, the small values of the prediction interval indicate that model predictions are reliable. Furthermore, the scatterplots and the standardized regression coefficients (SRC) show the relative importance and the existence of a linear relation between the uncertain parameters and the simulation results.

From the probability distribution of the output variables a comparison of the methods can be done. The assumption of a linear system behavior for the FOSM method could thus be confirmed.

In contrast to morphodynamic simulations, the analysis of steady state situation seems to be sufficient. The investigation of the temporal development of uncertainty is not necessarily needed as long as the objective of the study is not highly linked to flow development over time.

With the UnAnToPy tool it is very easy to set up an uncertainty analysis. In addition, the computing time required for the FOSM method for steady state scenarios should be negligible during calibration. Therefore, uncertainty quantification should be carried out as standard in order to enhance the reliability of the hydrodynamic modeling.

References

1. Altarejos-García L, Martínez-Chenoll ML, Escuder-Bueno I, Serrano-Lombillo A (2012) Assessing the impact of uncertainty on flood risk estimates with reliability analysis using 1-D and 2-D hydraulic models. Hydrol Earth Syst Sci 16:1895–1914. https://doi.org/10.5194/hess-16-1895-2012
2. Dalledonne GL, Kopmann R, Brudy-Zippelius T (2019) Uncertainty quantification of floodplain friction in hydrodynamic models. Hydrol Earth Syst Sci 23:3373–3385. https://doi.org/10.5194/hess-23-3373-2019
3. Koehler, J.R., Owen, A.B. (1996). Computer experiments, Handbook of Stat. S. Ghosh and C.R. Rao ed., Elsevier Science B.V. 13, 261–308.
4. Kopmann, R., Brudy-Zippelius, T. (2012). Using reliability methods for quantifying uncertainties in a 2D-morphodynamic numerical model of river Rhine. Proc. of the 2nd IAHR European Congress, 27. – 29.6.2012, TU München. Eds.: Peter Rutschmann, Markus Grünzner, Stephan Hötzl. München, ISBN 978–3–943683–03–5.
5. Kopmann, R., Dalledonne, G. (2021). Integration von Zuverlässigkeitsanalysen in die hydro- und morphodynamische Modellierung von Binnenwasserstraßen. BAW-FuE-Abschlussberichte Nr. B3953.05.04.70005, BAW, Karlsruhe.
6. Lindner, K. (1982). Der Strömungswiderstand von Pflanzenbeständen. Mitteilungen 75. Leichtweiss-Institut für Wasserbau, Technische Universität Braunschweig. (in German)
7. Merkel, U. (2018). Aufbau und Kalibrierung eines zweidimensionalen hydrodynamisch-numerischen Modells der Elbe zwischen Torgau und Wittenberg/L. Elbe-km 155 –220. Abschlussbericht. Unpublished.

8. Morgenschweis, G. (2011). Hydrometrie, Theorie und Praxis der Durchflussmessung in offenen Gerinnen. 582 S., 300 Abb., ISBN: 978–3–642–05389–4. Springer-Verlag.

9. Oubennaceur, K., Chokmani, K., Nastev, M., Tanguy, M., & Raymond, S. (2018). Uncertainty Analysis of a Two-Dimensional Hydraulic Model. Water 2018, 10, 272; doi:https://doi.org/10.3390/w10030272.

10. Walters, R. and Huyse, L. (2002). Uncertainty analysis for fluid mechanics with applications, Tech. Rep. 2002–1, Institute for Computer Applications in Science and Engineering, Hampton: ICASE, NASA Langley Research Center.

11. Warmink, J. J., & Booij, M. J. (2015). Uncertainty Analysis in River Modelling. Chapter in GeoPlanet: Earth and Planetary Sciences · July 2015. DOI: https://doi.org/10.1007/978-3-319-17719-9_11.